JOURNAL OF COMPUTATIONAL PHYSICS 77, 1–17 (1988)

An Effective Recursive Algorithm for Generating Many-Body Hugenholtz and Goldstone Diagrams

Z. CSÉPES AND J. PIPEK

Quantum Theory Group, Institute of Physics, Technical University, H-1521 Budapest, Hungary

Received February 20, 1987; revised July 9, 1987

A new recursive method for creating a general class of many-body diagrams (e.g., ground-state energy, open-shell, Bloch–Brandow, one- and two-particle Green-function, cluster operator) in Hugenholtz and Goldstone representation is described. The algorithm generates all linked and topologically distinct graphs up to arbitrary order of MBPT. Both one- and two-particle vertices can be taken into account. The procedure can be very effectively programmed for computer realization. The previous methods are discussed, results for non-Hartree–Fock vacuum diagrams are shown, and a procedure for the automatic evaluation of MBPT corrections using the Goldstone form of these graphs is presented. © 1988 Academic Press, Inc.

1. INTRODUCTION

Recently, a growing interest has been devoted to the investigation of electron correlation effects in small and middle-sized molecular systems using so-called "size-consistent" methods. "Size-consistence" means the proper physical behaviour of the calculated correlation energy when the number of particles (N) goes to infinity, and there exist numerous review articles [1–3] describing the generally used size-consistent "full configuration interaction" (full CI), "many-body perturbation theory" (MBPT) and "coupled-cluster theory" (CCT) methods. Unfortunately, for the full CI procedure the calculational efforts are increasing exponentially with the number of particles, while the complexity of MBPT and CCT is of polynomial order N on any given approximation level. It turned out [4] that CCT gives outstanding results even for low order approximation, but the exact treatment of the important four-particle (T_4 cluster) correlation effects, which arise only in higher orders of MBPT is completely out of the question in CCT, because of the inherent technical difficulties of the coupled-cluster method. However, Paldus and his group have recently published [4] an approximate method (ACPQ) for taking into account given types of diagrams of T_4 cluster corrections. The most promising procedure for treating moderately extended systems and at the same time for including higher order effects is MBPT. For detailed description of these theories we refer to the literature [2].

0021-9991/88 $3.00

In the preceding years very compact formulae were elaborated up to the fourth order in the perturbation theory using Wigner's $(2n+1)$ rule [5], but in the fifth order, where the T_4 corrections first appear, these expressions are not yet known. In this case the diagrammatic version of the MBPT can be used. Knowing the so-called Hugenholtz and Goldstone diagrams the algebraic form of the perturbation corrections can be easily constructed, since the combinatorial complexity of the problem is already solved by generating these graphs. On the other hand, the difficulties in drawing appropriate diagrams are growing extremely with the order of the perturbation theory and beyond the third order automatic generation is necessary.

The aim of this paper is to present an effective solution for this task, which can also be easily generalized for any kind of many-body diagrams. There already exist some algorithms to solve the problem of automatic diagram generation which will be discussed in Section 2. Section 3 defines the basic ideas and terminology used throughout this paper. In Section 4 we describe a much more effective algorithm than the existing ones, and in Section 5 a computer realization of our method is presented. The recognition of topologically equivalent diagrams is discussed in Section 6, and the automatic evaluation of MBPT corrections using our symbolic diagram representations is outlined in Section 7. Computational results for the so-called canonical and localized Hartree–Fock diagrams are shown in Section 8. Applications of our method for studying pair-energies, T_4 cluster corrections up to the fifth order [10], and the other electron correlation calculations using canonical and localized molecular orbitals [11] are described elsewhere.

2. Previous Methods for Diagram Generation

Paldus and Wong [6] elaborated the earliest method for generating all topologically distinct vacuum, one- and two-particle Green-function diagrams of a given order of MBPT. First they construct all topologically distinct Hugenholtz diagrams, but any one of them is regularly generated many times, since a considerable redundancy is yielded by their chosen mathematical description of a graph. Since they represent a diagram with a string of integers by passing through the vertices, there is no one-to-one correspondence between the strings and the diagrams. Using adjacency matrices for eliminating this redundancy is very laborious and this complication can be avoided by choosing an unambigous representation.

MBPT has been investigated from the point of view of group theory and combinatorial aspects [8, 9] and some effective methods for evaluating the number of Green and Goldstone graphs to estimate their contributions in any order of perturbation theory were developed [8, 12]. A classification of many-body diagrams is described [8, 9], and an appropriate representation for computer generation is also presented [8], but these results were not used for automatic evaluation of a graph contribution, so the efficiency of this method cannot be estimated.

Kaldor [7] elaborated another method for computer generating Goldstone and Bloch–Brandow diagrams; these latter ones are used in the degenerate MBPT. In the first step the so-called exchange sets, in fact the Hugenholtz graphs, are constructed and after contracting the Hermitian conjugated sets, the Goldstone diagrams are generated. Each Goldstone graph is determined by its loop structure. In this method the particle and hole lines are treated separately and an nth order exchange set in the case of two-particle vertices is represented with a string of $4n$ integers, which is twice as much as needed for an unambigous mathematical description. Since the generation rules for these integer strings are much less strict than that of the Hugenholtz diagrams, numerous strings are generated which do not correspond to valid graphs. A tedious validity test is necessary for eliminating the non-valid representations.

In Section 4 we show how these difficulties mentioned here can be avoided by choosing an appropriate representation which makes a one-to-one correspondence between integer strings and many-body diagrams. However, our method can be used effectively in the general case when all the diagrams up to a given order of MBPT are necessary, but if one wishes to generate a given type of graphs in a given order one would be better off with the existing programs [6] which enable a direct construction of such diagrams.

3. Basic Concepts of Hugenholtz and Goldstone Graphs

MBPT is based on the assumption that the total Hamiltonian H of the many-electron system can be split into two parts

$$H = H_0 + H_1, \tag{1}$$

where the eigenvalue problem of H_0 is solved and H_1 can be considered as a perturbation. The second quantized forms of these operators are as follows

$$H_0 = \sum_i \varepsilon_i c_i^\dagger c_i \tag{2}$$

$$H_1 = \sum_{i,j} \langle i|j\rangle\, c_i^\dagger c_j + \frac{1}{2} \sum_{i,j,k,l} \langle ij|kl\rangle\, c_i^\dagger c_j^\dagger c_l c_k \tag{3}$$

where $c_i^\dagger$ and c_i are the creation and annihilation operators, respectively. The expression of H_1 contains the matrix elements of the one- and two-particle interactions above a complete orthonormal basis set of the one-particle functions φ_i. Every expectation value can be determined by the Wick-algebra of the creation and annihilation operators and all members arising in the perturbation series correspond to a given graph. The rules of this correspondence are extensively discussed in the literature [2] and we shall repeat now only the most important results from our point of view. Two possible graphical representations will be described here, the Goldstone and the Hugenholtz diagrams.

A Goldstone diagram is constructed of vertices and directed fermion lines. In Fig. 1 the correspondence between the one- and two-particle Goldstone vertices and the interaction matrix elements can be seen. The two-particle vertex, denoted by two points joined with a dashed line, has one entering and one leaving directed fermion lines on both ends. The one-particle vertex, visualized by a crossed circle, has only one incoming and one outgoing fermion line.

A Goldstone diagram consists of ordered one- and two-particle vertices meanwhile some of their fermion lines may be joined and the rest remain free. The increasing order of the vertices, from right to the left, is called the "time-ordering" in the physical language and it determines the type (particle or hole) of the directed lines. Although it is important in the evaluation of the diagram contributions, on the generation and representation level these two types of the fermion lines can be treated equivalently, contrary to the method in Ref. [7]. A loop in a Goldstone diagram is a closed path created from directed lines. In this context the loop definition is different from that of in the graph theory. The knowledge of the loop structure is perhaps the most powerful tool for recognizing the equivalent Goldstone diagrams [8] arising in all generation procedures. In Section 5 we give a detailed description of its realization. Examples for simple loop structures can be seen in Fig. 2.

Due to the symmetry of the two-particle interaction any rotation of the two-particle vertices about a horizontal axis gives an equivalent diagram. From the point of view of the generation procedure and the automatic evaluation algorithm we also define the exchange set [7] of those Goldstone diagrams which can be obtained from each other by any exchange of the outgoing lines on given vertecies. An exchange set is represented by a Hugenholtz graph, which can be obtained from a Goldstone diagram by contracting the ends of the interaction lines to points. In the resulting graph there appear the so-called two-particle Hugenholtz vertices having two incoming and two outgoing fermion lines. Calculating with localized Hartree–Fock orbitals, as it is increasingly used in quantum chemical applications, a one-particle Hugenholtz vertex can be identified with a two-particle one having a

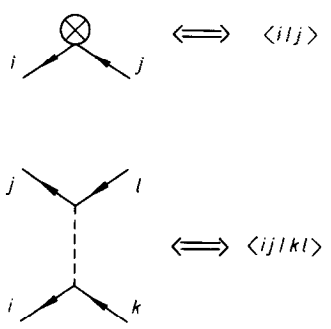

FIG. 1. The correspondence between the one- and two-particle Goldstone vertices and the interaction matrix elements.

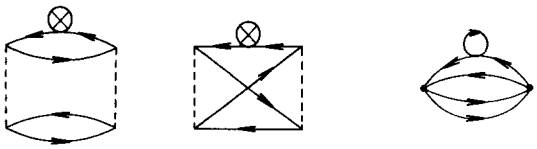

FIG. 2. An example for a third-order Hugenholtz graph with one bubble and the related "exchange set" of Goldstone diagrams.

"bubble." A bubble is a closed directed line on a two-particle vertex and we note that this construction is ordinarily called a loop in graph theory. In the following we use the term of bubble and reserve the loop definition given previously. Graphs with bubbles play an important role in the investigations of electron correlation problems [11, 13]. Two directed lines with common starting and ending vertices are considered equivalent. Figure 2 shows an example for an equivalent line pair and a bubble. The existence of equivalent line pairs in a Hugenholtz graph reduces the number of distinct Goldstone diagrams belonging to the given exchange set [2]. Connectivity can be defined as usual in the graph theory: a given gaph is connected if for any arbitrary two vertices there exists a path in the graph joining them. The ground state energy (so-called vacuum) diagrams have no free fermion lines. A graph is called linked if it does not contain a disconnected vacuum part. Due to this definition all linked ground-state energy diagrams are at the same time connected, too. As a consequence of the "linked-cluster" theorem [2, 3] we may deal only with the linked Hugenholtz graphs.

There are two important concepts which are generally used for classifying the graph contributions. Two Hugenholtz graphs are "Hermitian conjugated" if they can be obtained from each other by a reflection on a vertical axis keeping the original directions of the fermion lines. Using real one-particle orbitals the Hermitian conjugated graph pairs give the same contribution. On the other hand, a so-called "essential distinct" graph [6] represents a group of Hugeenholtz diagrams. Any two elements of this group can be obtained from each other by a given permutation of their vertices. It can be shown [10], that knowing the structure of every Hugenholtz diagram the CCT corrections can be uniquely separated in the perturbation expansion. On the other hand, using "essential distinct graphs" only, there is no one-to-one correspondence between these types of diagrams and CCT corrections. In order to make this separation possible we shall construct every Hugenholtz diagram.

4. REPRESENTATION INDEPENDENT GENERATION OF HUGENHOLTZ AND GOLDSTONE DIAGRAMS

In this section we shall describe a diagram generation algorithm which can, contrary to other existing methods [6, 7], be formulated on a completely abstract, graph theoretical level, without referring to any particular machine representation.

The method is applicable for generating all kinds (ground-state, open-shell, Bloch–Brandow, one- and two-particle Green-function, cluster operator) of *linked* many-body diagrams, which contain one- and two-particle electron interaction vertices. We follow the usual way, i.e., first generate all the Hugenholtz graphs in a given order, then the corresponding Goldstone diagrams by exchanging the fermion lines on the vertices.

A general nth order Hugenholtz diagram is a directed graph containing n electron interaction vertices labelled from 1 to n, as it was described in the previous section, and it is eventually completed by two virtual vertices labelled by 0 and ∞ if it is other than a ground-state diagram that we are talking about. The virtual vertices originally introduced by Paldus and Wong for Green-function diagrams [6] have different properties for each type of graphs, as it is shown in Table I.

TABLE I

Correspondence between Hugenholtz Diagram Types and Virtual Vertices

Object	Vertex ∞	Vertex 0	Graph
Ground-state energy	—	—	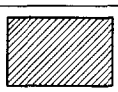
One-particle Green-function			
-hole	1 leaving line	1 entering line	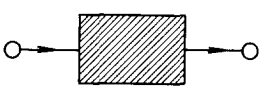
-particle	1 entering line	1 leaving line	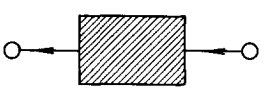
Two-particle Green-function			
-hole-hole	2 leaving lines	2 entering lines	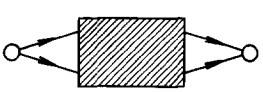
-particle-particle	2 entering lines	2 leaving lines	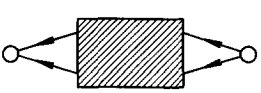
-particle-hole	1 entering and	1 entering and	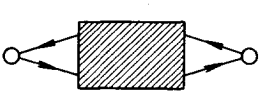
	1 leaving lines	1 leaving lines	
T_k Cluster operator	k entering and		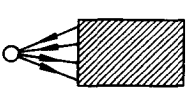
	k leaving lines	—	

Introducing virtual vertices has two definite advantages: on one hand each diagram containing free lines becomes a graph in the mathematical sense and each linked diagram become connected on the other hand.

A directed graph is defined by the set of its points and a set of arcs (directed lines) [14]. A directed line is an ordered pair of vertices (u, v), where the line enters the point u and leaves the point v, respectively. The most general nth order Hugenholtz graph contains the set of points $V = \{0, 1, ..., n, \infty\}$ and a set of lines $L = \{(u, v) | u, v \in V\}$, where each integer from 1 to n appears twice both in the first and second positions of (u, v), respectively. How many times the symbols 0 and ∞ appear in the ordered pairs depends on the number of entering and leaving lines of the virtual vertices. Let us now define two operations for an nth order Hugenholtz graph $h = \{V, L\}$:

(i) The operation $\oplus$ means the addition of the disconnected first-order two-electron vertex f as the point $(n+1)$ to h, as it is indicated in Fig. 3. Symbolically

$$f \oplus h = \{\oplus V, \oplus L\},$$

where

$$\oplus V = \{0, 1, ..., n, n+1, \infty\}$$

and

$$\oplus L = L \cup (n+1, n+1) \cup (n+1, n+1).$$

(ii) The operation $c(i, j)$ is defined for each pair of directed lines $i, j \in L$. Graphically it cuts the lines i and j, and joins the free end of the outgoing broken line originated from i to the free end of the incoming broken line originated from j, and vice versa (see Fig. 4). In the mathematical description

$$c(i, j)\, h = \{V, c(i, j)\, L\},$$

where

$$\begin{aligned} c(i, j)\, L &= c(i, j)\{\cdots i = (u, v) \cdots j = (x, y) \cdots\} \\ &= \{\cdots (u, y) \cdots (x, v) \cdots\}. \end{aligned}$$

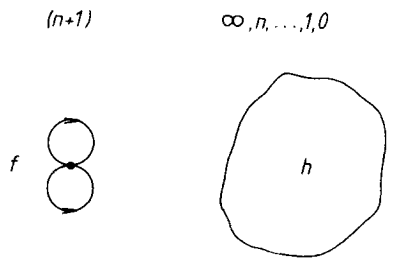

FIG. 3. The graphical representation of the operation $\oplus$ on an nth order Hugenholtz graph h.

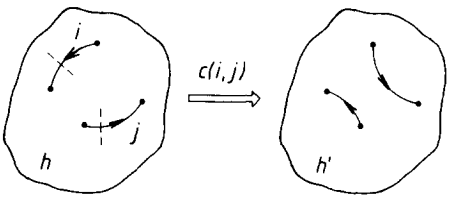

FIG. 4. The graphical representation of the operation $c(i,j)$ on an nth order Hugenholtz graph h yielding the graph h'.

We would like to mention here, that from the algorithmic point of view the $c(i,j)$ operation can be easily implemented by exchanging the second elements of the ordered pairs i and j. Clearly, both operations defined now do not change the number of incoming and outgoing lines of any vertices and so they result in valid (but not necessarily connected) Hugenholtz diagrams.

Let us consider now the combined operations

$$h_1 = c(i,j)[f \oplus h], \qquad \text{where} \quad i = (n+1, n+1), j \in L \tag{4}$$
$$h_2 = c(k,l)\, c(i,j)[f \oplus h],$$

where

$$i = (n+1,\ n+1),\ k = (n+1,\ n+1),\ j, l \in L. \tag{5}$$

According to our previous considerations we can trivially state

THEOREM 1. (a) *h_1 is a valid $(n+1)$th order Hugenholtz graph containing one bubble on the vertex $(n+1)$;*

(b) *h_2 is a valid $(n+1)$th order Hugenholtz graph with a usual two-electron vertex $(n+1)$.*

Since operations (4) and (5) join the disconnected first-order component f to the original graph h, the following holds.

THEOREM 2. *If the graph h is connected both the resulting h_1 and h_2 are connected, too.*

Proof. Let us consider first the graph h_1. All paths in h remain unaffected, except those, which connect the vertices a and b through the line $j = (x, y)$: $a \cdots x, y \cdots b$. In the new graph h_1 this path disappears, however, the new path $a \cdots x,\ (n+1),\ y \cdots b$ connects a and b again. Thus each connection between two arbitrary vertices of h is still kept. On the other hand, the new vertex $(n+1)$ is joined to every other vertex in h, since for an arbitrary vertex a in h there must exist a path $a \cdots x$ and in the new graph h_1 the path $a \cdots x\ (n+1)$ joins a with $(n+1)$. In the case of h_2 this proof must be repeated twice.

From the point of view of our generation procedure the most important result is that all $(n+1)$th order connected Hugenholtz diagrams can be generated from nth order connected ones using procedures (4) and (5).

THEOREM 3. *For each $(n+1)$th order connected Hugenholtz graph $h^{(n+1)}$ there exists at least one nth order connected graph h that $h^{(n+1)} = h_1$ or $h^{(n+1)} = h_2$ defined in* (4) *and* (5), *respectively.*

Proof. Let us start with the easier case when the vertex $(n+1)$ of $h^{(n+1)}$ contains a bubble. Clearly, in this case the procedure (4) is applicable. Now, the lines $(n+1, x)$ and $(y, n+1)$ join the vertex $(n+1)$ to the other parts of the diagram. Following now the opposite way used in procedure (4) let us separate the vertex $(n+1)$ and join the line $(n+1, x)$ with $(y, n+1)$ creating $j=(x, y)$. The resulting nth order graph h is clearly a valid Hugenholtz diagram and all connections of the type $a \cdots x$, $(n+1)$, $y \cdots b$ are still kept through the path $a \cdots x$, $y \cdots b$, i.e., h is connected. In other words operation (4) is invertible. When the point $(n+1)$ is a two-electron vertex the procedure (5) must be used. Unfortunately, separating the vertex $(n+1)$ now the two line pairs $(u, n+1)$, $(n+1, v)$, $(x, n+1)$, $(n+1, y)$ can be joined in two different ways: $j=(u, v)$ and $l=(x, y)$ or $j=(u, y)$ and $l=(x, v)$. Therefore, there is no unique inverse for operation (5) and $h^{(n+1)}$ can be generated from two different nth order valid Hugenholtz graphs h' and h''. We shall show now that at least one of them is connected. It is easy to understand that if h' containing the lines (u, v) and (x, y) is disconnected it may not consist of more than two disconnected components, since $h^{(n+1)}$ is connected and procedure (5) can join at most two components. It is also clear that the lines $j=(u, v)$ and $l=(x, y)$ must be in different disconnected parts, otherwise operation (5) would again result in a disconnected $(n+1)$th order Hugenholtz graph. From this it follows that for an arbitrary vertex a a path $a \cdots u$ must exist in the first connected component and for an arbitrary vertex b in the second component a path $y \cdots b$, must exist, respectively. Consequently, in the graph h'' containing the lines $j=(u, y)$, $l=(x, v)$ the points a and b are joined through the path $a \cdots u$, $y \cdots b$ and thus h'' is connected.

We are now in the position to define a recursive algorithm for the generation of all valid and connected $(n+1)$th order Hugenholtz diagrams: knowing the set of all connected, topologically distinct nth order Hugenholtz diagrams let us apply operations (4) and (5) to all members of the set running the lines j and l over the whole graph including those ones, too, which form a bubble or start or end on virtual vertices.

According to Theorem 3 we can create in this way all topologically distinct connected diagrams appearing in the $(n+1)$th order. On the other hand, some diagrams can be generated more than one (if equivalent lines are cut in procedures (4) and (5) or the original nth order diagrams h' and h'' introduced in the proof of Theorem 3 are both connected). For this reason we need a procedure to select the equivalent Hugenholtz diagrams, but we shall see in Section 6 that, using an appropriate representation, this step becomes trivial. Finally, we wish to remark the

following. An argument similar to the proof of Theorem 3 shows that in order to obtain $(n+1)$th order diagrams without bubbles in the nth order all connected graphs containing bubbles are necessary, too. In a given order such linked diagrams which become disconnected by removing the virtual vertices are also necessary for the generation of some connected and linked graphs with free lines in the next order. These facts show that the class of diagrams considered by us is the minimum set for generating all linked Hugenholtz diagrams in an arbitrary order.

The generation of Goldstone diagrams belonging to an exchange set is quite straightforward from a given Hugenholtz diagram. As we have mentioned earlier a two-electron Hugenholtz vertex appears twice, on the first and on the second position of the directed lines (u, v), respectively. Let us suffix an additional quantity to the vertices of such lines:

$$(u, v) \to (u, \alpha \mid v, \beta), \qquad \text{where } \alpha, \beta = 1 \text{ or } 2 \tag{6}$$

describing the fact that the Goldstone line enters the αth end of the two-electron vertex u and originates on the βth end of the vertex v. Since the Goldstone two-electron vertices can be freely rotated around the horizontal axis we can choose, without restricting generality, the suffix 1 to the first occurrence of u on the left-hand side and the suffix 2 for the second one. The two appearances of v on the right-hand side of the Goldstone line (6) (outgoing lines) must be labelled by the numbers 1 and 2 and by an exchange 2 and 1, respectively. These two possibilities for every two-electron vertex yield 2^{n-m} Goldstone diagrams belonging to the given nth order exchange set (m is the number of one-electron vertices. If the Hugenholtz graph contains equivalent lines there appear topologically equivalent Goldstone diagrams in the exchange set. The recognition of these graphs is described in Section 6.

5. Computer Representation of Hugenholtz and Goldstone Diagrams

As described in Section 4, an nth order Hugenholtz graph is represented by a set of ordered pairs

$$\{(1, x_1), (1, y_1), \ldots, (n, x_n), (n, y_n)\}; x_i \leqslant y_i \qquad (i = 1, \ldots, n), \tag{7}$$

where x_i and y_i correspond to Hugenholtz vertices. We shall identify a Hugenholtz diagram with a string of integers consisting of these x_i and y_i numbers. $H = x_1 y_1 \cdots x_n y_n$ is called the Hugenholtz index. H can be interpreted as an integer number in a numeration system based on $(n+1)$ and in the computer realization this number is stored in one or more integer variables depending on the computer word length. The Hugenholtz graph shown in Fig. 2 has the index $H = 331212$. It

can be easily seen that this is an unambigous representation of the Hugenholtz diagram. The operations defined in Section 4 can be realized in a simple way:

$$\oplus\{(1, x_1), (1, y_1), ..., (n, x_n), (n, y_n)\}$$
$$= \{(1, x_1), ..., (n, y_n), (n+1, n+1), (n+1, n+1)\} \tag{8}$$

and

$$\oplus H = x_1 y_1 \cdots x_n y_n (n+1)(n+1). \tag{9}$$

The $c(i, j)$ operation means the exchange of the second elements of the ith and jth ordered pairs, considering the requirements $x_i \leqslant y_i$ and $x_j \leqslant y_j$. As it was shown in Section 4, a Goldstone diagram is represented by a set of the $(u\alpha \mid v\beta)$ quantities:

$$(11 \mid x_1\alpha_1), (12 \mid y_1\beta_1), ..., (n1 \mid x_n\alpha_n), (n2 \mid y_n\beta_n),$$

where $\alpha_i, \beta_i = 1, 2.$ (10)

Thus we can simply represent a Goldstone diagram by two strings of integers. One of these quantities is the Hugenholtz index $H = x_1 y_1 \cdots x_n y_n$, and the other will be called the Goldstone index $G = \alpha_1\beta_1 \cdots \alpha_n\beta_n$. An exchange of the outgoing lines on any vertex results in changing two quantities α or β to $(3-\alpha)$ or $(3-\beta)$, which makes the generation of the exchange sets very fast. The recognition procedure of the equivalent Goldstone graphs based on the loop structure will be discussed in the next section.

6. Recognition of Topologically Equivalent Diagrams

The identification of equivalent Hugenholtz graphs originated from the generation procedure is very simple owing to the one-to-one correspondence between the graphs and the chosen representation. The equivalence of two Hugenholtz diagrams can be settled by a simple arithmetic comparison of their representing indices.

In the case of equivalent Goldstone diagrams the situation is more complicated. Although our representation is very convenient for generation purposes, it does not realize a unique mapping of Goldstone diagrams. We shall show now how to create a simple number which is in a one-to-one correspondence with a given Goldstone diagram.

We utilize the fact that these kinds of graphs can be unambigously represented by the set of their loops [8]. Using the Goldstone representation from Section 5 the

$$(u, \alpha \mid v, \beta)$$

directed lines are unambigously defined. Let us pass through the first loop in the graph starting at the largest Hugenholtz vertex number (∞ or n). The path can be

easily followed in the reverse direction using the chosen Goldstone representation. Let us record the Hugenholtz vertices (i.e., dropping the α or β suffixes) in their order of occurrence in the walk along the loop and remove all the traversed Goldstone line of the walk.

Thus the first loop is represented by a string of integers $r_1 = a_1 b_1 \cdots z_1$ which can be treated as an integer in a numeration system based on $(n+1)$. The second loop can be started at the next largest vertex where an unttouched line enters, constructing $r_2 = a_2 b_2 \cdots z_2$, and so on. The next step is to sort the $r_i (i = 1 \cdots l)$ strings according to their numerical value into an ascending order $r'_1 r'_2 \cdots r'_l$ where $r'_1 \geqslant r'_2 \geqslant \cdots r'_l$, l means here the number of loops in the Goldstone diagram. Adding the length n_i of the loop i to the string r'_i we can form the following block of integers:

$$b = l n_1 r'_1 n_2 r'_2 \cdots n_l r'_l.$$

It is easy to see that from b we can reproduce the r'_i loops as it is usual in the file handling for variable length blocked records. The procedure given now maps a Goldstone graph unambigously to the block of integers b. All equivalent diagrams result in the same b. On the other hand, b unambigously determines the loop structure which distinguishes non-equivalent diagrams. Now creating the integer strings b_1 and b_2 for two Goldstone graphs their equivalence can be checked easily by finding $b_1 = b_2$.

7. Automatic Evaluation of MBPT Corrections

There is a one-to-one correspondence between a member of the many-body perturbation series and a given Goldstone diagram. We restrict ourselves to give an automatic evaluation procedure for the closed-shell ground-state energy diagram contributions only; the generalization for other graphs can be easily made.

Each Goldstone diagram corresponds to a sum arising in the energy expansion. In the spin-free formalism the evaluation rules are as follows:

(i) Every fermion line carries an index.

(ii) One- and two particle vertices are to be substituted by off-diagonal Fock-matrix elements and two-electron integrals, respectively, as indicated in Fig. 1.

(iii) Each diagram has a topological factor $(-1)^{l+h} 2^l w_\Gamma$. And

(iv) two subsequent vertices determine an energy denominator where l is the number of the loops and h is the number of the hole lines, respectively. To define w_Γ we have to note the following. If an nth order Hugenholtz graph contains m bubbles and p equivalent line pairs, there are 2^{n-m-p} non-equivalent Goldstone diagrams belonging to this exchange set. In this case for each distinct Goldstone diagrams w_Γ equals 1. In the case of nth order Hugenholtz graphs without bubbles, which have the maximum number n equivalent line pairs only two non-equivalent

Goldstone diagrams belong to the exchange set and each of them carries the factor $w_\Gamma = \frac{1}{2}$ [5].

A diagram contribution can be determined in the following way. Composing the product of all the n matrix elements and dividing it by the product of $n-1$ energy expressions, one must sum up all the indices and multiply the result with the topological factor in which 2^l expresses the result of the summation for the spin-variables [2].

An energy expression can be constructed by considering the fermion lines between two subsequent vertices in the diagram as follows

$$D = \varepsilon_{h_1} + \varepsilon_{h_2} + \cdots + \varepsilon_{h_k} - \varepsilon_{p_1} - \varepsilon_{p_2} - \cdots - \varepsilon_{p_k},$$

where h_i and p_i denote the indices of the hole and particle lines, respectively. The first Goldstone diagram in Fig. 2 yields the contribution

$$(-1)^{2+2} \times 2^2 \sum_{\substack{h_1 h_2 \\ p_1 p_2 p_3}} \frac{\langle p_1 p_2 | h_1 h_2 \rangle \langle p_3 | p_2 \rangle \langle h_1 h_2 | p_1 p_3 \rangle}{D_1 \times D_2},$$

where $D_1 = \varepsilon_{h_1} + \varepsilon_{h_2} - \varepsilon_{p_1} - \varepsilon_{p_2}$ and $D_2 = \varepsilon_{h_1} + \varepsilon_{h_2} - \varepsilon_{p_1} - \varepsilon_{p_3}$.

In an nth order Goldstone diagram with labelled vertices the fermion lines are given by the set of $(u\alpha | v\beta)$ quantities, as described in the previous sections. (For the virtual and one-particle vertices the suffix always equals 1.) In the case of equivalent lines the Hugenholtz set contains two equal (u, v) pairs. The number of loops can be determined as shown in Section 5. The type of directed line can be easily determined by the difference $u - v$. If $u - v > 0$ the line is of a particle type and in the case $u - v < 0$ it means the whole line. In the Hugenholtz representation $u = v$ means a bubble and this line is ignored during the evaluation of the related Goldstone diagram contributions.

Knowing the Goldstone set of $(u\alpha | v\beta)$ quantities a trivial labelling of the fermion lines can be made. Every matrix element can be symbolically represented by the label set of the incoming and outgoing lines. Owing to this, every energy expression can be constructed symbolically, too. Starting with the first vertex one can write $D_1 = \varepsilon_{h_1} + \varepsilon_{h_2} - \varepsilon_{p_1} - \varepsilon_{p_2}$, where h_i and p_i are the labels of the entering and leaving lines, respectively. In the next step $D_2 = D_1 + (\varepsilon_{i_1} + \varepsilon_{i_2} - \varepsilon_{j_1} - \varepsilon_{j_2})$ where i_k and j_k are the symbolic labels of the incoming and outgoing lines of the second vertex, respectively. Following this procedure each energy expression can be constructed. In the computer realization the actual machine addresses of the matrix elements and the ε_i quantities are evaluated on the basis of this symbolical representation. Generating the Goldstone set of $(u\alpha | v\beta)$ quantities the topological factor can be easily determined.

Of course, some simplifications can be made on the level of the Hugenholtz graphs, contracting the Hermitian conjugated diagrams as in Ref. [7] and creating optimization classes with the change of the fermion line labelling, but we do not

treat these questions here. A complete fifth-order calculation for the correlation energy based on this method will be published elsewhere [10].

Our automatic evaluation method involves straightforward summation over all indices. Wigner's $(2n+1)$ rule provides a more effective tool for determining the correlation energy up to and including the fourth-order of MBPT [5], but the exact formulae based on Wigner's $(2n+1)$ rule are not yet known for the complete higher order MBPT corrections. Considering this fact the automatic evaluation method presented here could be a reference for checking other sophisticated methods might be developed in the future; on the other hand, it is appropriate for the calculation of the complete fifth-order correlation energy correction of some simple systems [10].

8. Computational Results

Based on the general algorithm described in the previous sections, we have elaborated a new program for generating any kind of many-body diagrams contained in Table I. Theoretically the method can be applied up to an arbitrary order of MBPT; in practice, however, the time consumption and storage requirements increase extremely with the order of the perturbation theory.

In quantum chemistry the BMPT is commonly used for the evaluation of the correlation energy. We present here the results of an illustrative calculation for those kind of many-body ground-state diagrams (see the first entry in Table I) which appear in this problem. There are two different types, the so-called canonical and localization diagrams, respectively [13]. The canonical graphs do not contain any bubble at all; on the other hand, in the localization diagrams the one-particle

TABLE II

The Number of the Canonical Diagrams up to the Fifth Order of Perturbation Theory

n^a	N_H^b	N_G^c	N_{CH}^d	N_{CG}^e
2	1	2	1	2
3	3	12	3	12
4	39	300	31	242
5	840	13,680	462	7552

[a] The order of perturbation theory.

[b] The number of Hugenholtz graphs before contracting the Hermitian conjugated pairs.

[c] The number of Goldstone diagrams belonging to the N_H exchange sets.

[d] The number of Hugenholtz graphs after contracting the Hermitian conjugated pairs.

[e] The number of Goldstone diagrams belonging to the N_{CH} exchange sets.

vertices (represented by bubbles) must have the same type of incoming and outgoing fermion lines. As a simple consequence of this fact the localization diagrams may not contain bubbles on the end vertices. The program creates all the distinct graphs with bubbles and after a validity test only the localization diagrams are kept.

On evaluating the correlation energy the Hermitian conjugated graphs give the same contribution, thus it is worth contracting them on the calculation level. On the other hand, if one wishes to analyze the CCT contributions, each diagram must be distinguished. At present, complete correlation energy calculations can be carried out only up to and including the fifth order of MBPT [10]; the higher order calculations due to the calculational difficulties are completely out of question. Considering this fact, we present our results for diagram generation up to the fifth order of MBPT. Table II and Table III show the number of canonical and localization Hugenholtz (N_H) and Goldstone (N_G) diagrams. We have also contracted the Hermitian conjugated Hugenholtz (N_{CH}) diagrams. N_{CG} stands for the number of the Goldstone diagrams in the exchange sets belonging to the contracted Hugenholtz graphs.

Since the order of the contribution of a given localization graph depends on the number of one- and two-particle vertices [11]; it is worth separating the diagrams according to their bubble-number. Table IV shows the number of the localization Hugenholtz and Goldstone diagrams before and after contracting the Hermitian conjugated Hugenholtz graphs.

TABLE III

The Number of the Localization Diagrams up to the Fifth Order of Perturbation Theory

n^a	N_H^b	N_G^c	N_{CH}^d	N_{CH}^e
3	2	4	2	4
4	22	96	13	52
5	522	4464	300	2532

[a] The order of perturbation theory.

[b] The number of Hugenholtz graphs before contracting the Hermitian conjugated pairs.

[c] The number of Goldstone diagrams belonging to the N_H exchange sets.

[d] The number of Hugenholtz graphs after contracting the Hermitian conjugated pairs.

[e] The number of Goldstone diagrams belonging to the N_{CH} exchange sets.

TABLE IV

The Number of the Localization Diagrams up to the Fifth Order of Perturbation Theory after Separation by the Number of Bubbles

n^a	N_B^b	N_H^c	N_G^d	N_{CH}^e	N_{CG}^f
3	1	2	4	2	4
4	1	16	80	8	40
	2	6	16	5	12
5	1	420	3920	240	2224
	2	82	480	46	264
	3	20	64	14	44

[a] The order of perturbation theory.
[b] The number of bubbles in the Hugenholtz graphs.
[c] The number of Hugenholtz graphs before contracting the Hermitian conjugated pairs.
[d] The number of Goldstone diagrams belonging to the N_H exchange sets.
[e] The number of Hugenholtz graphs after contracting the Hermitian conjugated pairs.
[f] The number of Goldstone diagrams belonging to the N_{CH} excange sets.

REFERENCES

1. B. ROOS, in *Computational Techniques in Quantum Chemistry and Molecular Physics*, edited by Diercksen *et al.* (Reidel, Dordrecht, 1975), p. 251; I. SHAVITT, in *Modern Theoretical Chemistry*, edited by H. F. Schaefer (Plenum, New York, 1977), Vol. 3, p. 189; R. J. BARTLETT AND G. D. PURVIS, *Int. J. Quantum Chem.* **14**, 561 (1978).
2. A. L. FETTER AND J. D. WALECKA, *Quantum Theory of Many-Particle Systems* (McGraw–Hill, New York, 1971); J. PALDUS AND J. CIZEK, *Adv. Quantum Chem.* **9**, 105 (1975); S. WILSON, in *Theoretical Chemistry* (The Royal Society of Chemistry, London, 1981), Vol. 4, p. 1.
3. J. CIZEK, *J. Chem. Phys.* **45**, 4256 (1966); J. CIZEK, *Adv. Chem. Phys.* **14**, 35 (1969); V. KVASNICKA, V. LAURINC, S. BISKUPIC, AND M. HARING, *Adv. Chem. Phys.* **52**, 181 (1983); J. PALDUS, in *New Horizons of Quantum Chemistry*, edited by P-O. Löwdin and B. Pullman (Reidel, Dordrecht, 1983), p. 31; R. J. BARTLETT, C. E. DYKSTRA, AND J. PALDUS, in *Advanced Theories and Computational Approaches to the Electronic Structure of Molecules*, edited by C. E. Dykstra (Reidel, Dordrecht, 1984), p. 127.
4. J. PALDUS, M. TAKAHASHI, AND R. W. H. CHO, *Phys. Rev. B* **30**, 4267 (1984); J. PALDUS, J. CIZEK, AND M. TAKAHASHI, *Phys. Rev. A* **30**, 2193 (1984); M. TAKAHASHI AND J. PALDUS, *Phys. Rev. B* **31**, 5121 (1985); W. FÖRNER, J. CIZEK, P. OTTO, J. LADIK, AND O. E. STEINBORN, *Chem. Phys.* **97**, 235 (1985); W. FÖRNER, J. LADIK, P. OTTO, AND J. CIZEK, *Chem. Phys.* **97**, 251 (1985); M. TAKAHASHI AND J. PALDUS, *Int. J. Quantum Chem.* **28**, 459 (1985).
5. V. KVASNICKA, V. LAURINC, AND S. BISKUPIC, *Mol. Phys.* **39**, 143 (1980); V. KVASNICKA, V. LAURINC, AND S. BISKUPIC, *Czech. J. Phys. B* **31**, 41 (1981).
6. J. PALDUS AND H. C. WONG, *Comput. Phys. Commun.* **6**, 1 (1973); H. C. WONG AND J. PALDUS, *Comput. Phys. Commun.* **6**, 9 (1973).
7. U. KALDOR, *J. Comput. Phys.* **20**, 432 (1976).
8. G. ROSENSTEEL, E. IHRIG, AND L. E. H. TRAINOR, *Proc. R. Soc. A* **344**, 387 (1975); E. IHRIG, G. ROSENSTEEL, H. CHOW, AND L. E. H. TRAINOR, *Proc. R. Soc. A* **348**, 339 (1976).
9. V. KVASNICKA, *Int. J. Quantum Chem.* **21**, 1003 (1982).

10. Z. CZÉPES AND E. KAPUY, to be published.
11. J. PIPEK AND J. LADIK, *Chem. Phys.* **102**, 445 (1986).
12. A. E. JACOBS, *Phys. Rev. D* **23**, 1760 (1981); F. BATTAGLIA AND T. F. GEORGE, *J. Math. Phys.* **25**, 3489 (1984).
13. S. DINER, J. P. MALRIEU, AND P. CLAVERIE, *Theor. Chim. Acta* **13**, No. 1, 18 (1969); A. T. AMOS AND J. I. MUSHER, *J. Chem. Phys.* **54**, 2380 (1971); E. R. DAVIDSON, *J. Chem. Phys.* **57**, 1999 (1972); E. R. DAVIDSON AND C. F. BENDER, *J. Chem. Phys.* **56**, 4334 (1972); E. KAPUY, Z. CSÉPES, AND C. KOZMUTZA, *Int. J. Quantum Chem.* **23**, 981 (1983).
14. F. HARARY, "Graph Theory" (Addison–Wesley, Reading, MA, 1969).